

Structural and transport properties in solid-state conducting gels: influence of the crosslink density

B. Pépin-Donat^a, A. de Geyer^b and A. Viallat^{c,*}

^aLaboratoire de Physique des Métaux Synthétiques, U.M.R. 585 (CEA-CNRS-Université J. Fourier), Département de Recherche Fondamentale sur la Matière Condensée, CEA-Grenoble, 17 Av. des Martyrs, 38054 Grenoble Cedex 9, France

^bLaboratoire de Physico-Chimie Moléculaire, U.M.R. 585 (CEA-CNRS-Université J. Fourier), Département de Recherche Fondamentale sur la Matière Condensée, CEA-Grenoble, 17 Av. des Martyrs, 38054 Grenoble Cedex 9, France

^cLaboratoire de Spectrométrie Physique, Université J. Fourier, CNRS (UMR C588), BP 87, 38402 St Martin d'Hères Cedex, France
 (Revised 13 February 1998)

Solid-state properties of undoped gels of poly(3-*n*-octylthiophene) (POT) are investigated by N₂ BET surface measurements, X-ray diffraction and small-angle X-ray scattering (SAXS) experiments. The observed variations in compacity, crystalline domain sizes and typical sizes of large-scale heterogeneities *versus* the crosslink ratio, R_i , all exhibit an extremum for the gel $R_i = 1/100$. As reported earlier, this gel in the doped state also exhibits the highest conductivity. A major interest in the crosslinking process is to enhance the conductivity by modifying POT crystallinity. A deeper understanding of the crystallization mechanisms should therefore allow one to master the transport properties in POT systems. © 1998 Elsevier Science Ltd. All rights reserved.

(Keywords: conducting gels; solid-state structure; poly(alkylthiophene))

Introduction

This work concerns the solid-state properties of unswollen fully conjugated poly(3-*n*-octylthiophene) (POT) gels prepared from oxidative copolymerization of tri(2'-thienyl)-1,3,5-benzene units with octylthiophene units.

In previous work¹, the statistical structure of these gels studied above the chain melting temperature has been described by a single variable characterizing the physical state of gelation, fR_i , where f is the gel functionality and R_i the molar ratio crosslinks/octylthiophene units. A progressive and monotonous tightening of the gel mesh size has been observed upon increasing the crosslink concentration, as could be expected from the classical theories of polymer gelation.

On the other hand, the study of the transport properties of the doped networks² has disclosed that the highest room temperature conductivity is observed for the gel of molar crosslink ratio $R_i = 1/100$ (Figure 1). Moreover, the variations of conductivity *versus* temperature, which have been satisfactorily interpreted using an inter-conducting clusters hopping model, have shown that the diameters of mean conducting-clusters also present a maximum value for the gel $R_i = 1/100$.

These results show that the physical origin of the variations of conductivity *versus* R_i cannot be readily related to the primary intrinsic topological structure of the gels. Thus, if a correlation between conductivity and solid-state chain structure exists, as is regularly questioned in the literature, it must involve a secondary structure characteristic of solid polymers, i.e. the semi-crystalline state, and must imply a dependence of the crystallinity on R_i . In order to clarify this point, we have undertaken a thorough study of crystallization processes in POT gels and we report here the first results.

Experimental

Six networks were prepared starting from different initial molar ratios $R_i = 1/15, 1/30, 1/50, 1/100, 1/200, 1/500$. Each copolymerization reaction leads to a soluble and an insoluble fraction. This paper only deals with the insoluble fractions (gels).

Conductivity measurements were performed on doped samples. Doping was achieved in a 1 M solution of FeCl₃·6H₂O in nitromethane. The doped samples were then washed with acetonitrile, dried under vacuum at room temperature and reweighed to determine the amount of dopant uptake. The molar doping levels are around 20%. The doped samples were pressed as pellets, 7 mm in diameter and about 0.5 mm thick. The room temperature conductivity was measured by the collinear four-point probe method³. The experimental part related to doping, room temperature and variable (low) temperature dc conductivity and thermoelectric power measurements are reported in detail in Ref. 2.

X-ray diffractions were measured with a home-made diffractometer with a micro-control goniometer (precision: 0.002° (2θ)) using graphite crystal monochromatized Cu Kα radiation (λ = 1.542 Å) (50 kW, 20 mA tube) and a scintillation point detector. All diffraction profiles were measured in reflection mode by a θ–2θ scan. Data were obtained from 2 to 50° (2θ) at a scan rate of 0.05° min⁻¹. The spectra were then fitted with a sub-programme FIT of DIFFRACT AT (Socabim-Siemens); split-common functions were used. Samples were pressed as pellets of 7 mm diameter (approximately 0.5 mm depth) and glued onto the sample holder. The samples were observed without any preliminary thermal treatment.

N₂ BET surfaces were measured on an AccuSorb 2100E (Micrometrics) physical adsorption analyser. Samples were first degassed at 60°C for 20 h. The deadspace was determined

*To whom correspondence should be addressed

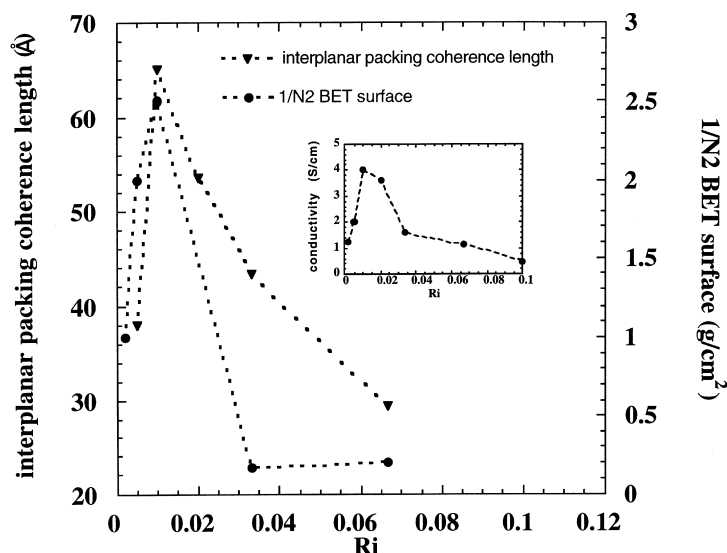


Figure 1 Evolution of room temperature conductivity, N_2 BET surface and interplanar packing coherence length with R_i

using a non-adsorbing gas, helium, at the temperature of the subsequent N_2 adsorption test (approximately 77 K). Three N_2 adsorption measurements were performed at relative pressures of 0.1, 0.2 and 0.3% with respect to the N_2 saturating pressure. Specific surfaces were obtained from the values of equilibrium pressures according to the standard method described in Ref. 4.

Small-angle X-ray scattering (SAXS) experiments were performed at the European Synchrotron Radiation Facilities (ESRF, Grenoble, France) using the SAXS instrument available at the D2AM beam line⁵. The scattered intensity was measured over a range of scattering vectors $5 \times 10^{-3} \text{ \AA}^{-1} < Q < 0.1 \text{ \AA}^{-1}$, $Q = (4\pi/\lambda) \sin \theta$ where 2θ is the total scattering angle and λ is the wavelength ($\lambda = 1.54 \text{ \AA}$). The scattering curves were measured using a point focusing geometry and a linear gas-filled detector at a sample-to-detector distance of 2 m. Experimental intensities (arbitrary units) corrected for the incoming flux and the background scattering from the empty beam were normalized to the same sample thickness.

Results

Size of crystalline domains. The diffraction profile observed on linear POT chains is the same as that reported in the literature⁶. Similar profiles are obtained for the networks: all spectra present four crystalline peaks (position (2θ) around 4, 8, 12 and 23°) and two amorphous ones (position (2θ) around 20 and 40°). The first three crystalline peaks (around 4, 8 and 12° (2θ)) represent the first-, second- and third-order reflections, respectively, of the $\approx 21 \text{ \AA}$ one-layer packing (intraplanar) repeat. This intraplanar packing is formed by intercalation of the side-chains between two neighbouring coplanar main chains. The high angle crystalline peak (around 23° (2θ)) is representative of an approximate interplanar stack repeat of 3.7 \AA (interplanar packing). The coherence lengths of the different crystalline domains have been evaluated from the Sherrer equation⁷. We observe a maximum of the interplanar packing coherence length for the sample of crosslink concentration $R_i = 1/100$ (Figure 1).

In all cases, the crystallinity of these gels is weak which makes the quantitative determination of the crystallinity

ratios difficult from the observation of peaks of diffraction (the presence of broad amorphous peaks). Nevertheless, we clearly observe that the crystallinity ratio of gels of $R_i \geq 1/50$ increases with decreasing R_i . The crystallinity ratios of gels of $R_i \leq 1/100$ are unambiguously higher than the previous ones but within this range of crosslink concentration no clear evolution of these ratios *versus* R_i can be drawn.

Compacity. N_2 BET measurements performed on undoped gels yield the specific surface of the samples, corrected for the contribution of interstitial volumes. The results are presented in Figure 1. The variation of the surface with the crosslink concentration exhibits a minimum for POT linear chains and for the gel of crosslink concentration 1/100, i.e. the compacity is maximum for these two systems. The gels whose crystalline domains are the largest present the smallest BET surfaces, as it was naively expected since crystalline domains are generally more compact than amorphous ones.

Large-scale heterogeneous structures. Small-angle X-ray scattering spectra obtained on the gels are represented in Figure 2. The intensity obeys a power law $I(Q) \approx Q^{-n}$, whatever the crosslink concentration of the studied gel. The slope decreases with the crosslink concentration: $n = 3.5$ for $R_i = 1/15$ and $n = 3.2$ for POT. The diffusion is due to the internal surface of large-scale heterogeneities which may reveal the microgel structure of these systems. The deviation from the Porod law ($I \approx Q^{-4}$) suggests that the heterogeneities' interfaces present an irregular structure. Over the range $R_i = 1/30$ to $1/500$, the slope remains constant with a value $n = 3.3$, thus allowing comparison of the limiting values $I(Q)Q^n$ for the gels formed at these intermediate concentrations.

The diffusion in the Porod range depends on the specific surfaces of the heterogeneities and on the contrast $\Delta\rho^2$. If we assume that the contrast is essentially due to the difference between crystalline and amorphous densities and according to the observed evolution of the crystallinity ratio *versus* R_i evoked above, the limiting value $I(Q)Q^n$, proportional to $\Delta\rho^2$, should increase as R_i decreases. It is the reverse which is observed, thus suggesting an important change in the specific surface of the samples.

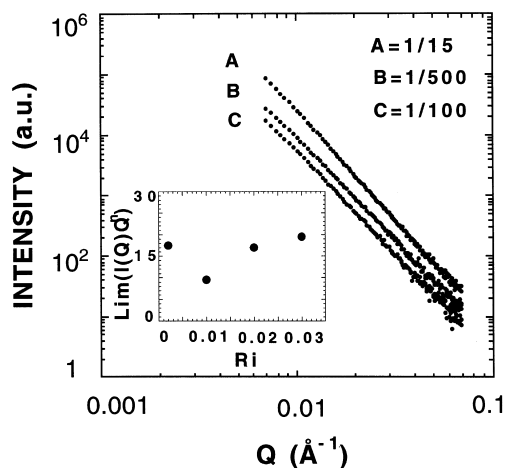


Figure 2 Scattering curves $\log I$ versus $\log Q$ for POT gels at different crosslink concentrations $R_i = 1/15, 1/100, 1/500$, showing power law $I(Q) \approx Q^{-n}$. A slope $n = -3.3$ is found for concentrations $R_i = 1/30, 1/100, 1/200$ and $1/500$. The inset displays $\lim [I(Q)Q^n]$ for these four R_i values and shows a minimum for gel 1/100

The scattered intensity of the various gels is minimum for the sample of crosslink concentration $R_i = 1/100$. The observed minimum of $\lim [I(Q)Q^n]$ in Figure 2 suggests that the surface per unit of volume associated with the heterogeneities goes through a minimum for this latter gel. This result might be seen either as a maximum of the size of heterogeneities or as better connected heterogeneities in the gel 1/100. The extremum observed for the gel 1/100 suggests that large-scale heterogeneities and crystalline domains are correlated although crystalline domain sizes ($\approx 100 \text{ \AA}$) are much smaller than heterogeneities sizes measured by SAXS. This point should be clarified by complementary SAXS measurements conducted on systems above the melting temperature.

Discussion

The variations versus R_i of crystalline domain sizes, compacity, X-ray scattered intensity, conductivity and sizes of conducting islands all present an extremum for the value $R_i = 1/100$. These quantities seem therefore to be correlated, although structural and transport properties are measured on systems in different physical states (undoped or doped).

In order to quantitatively establish these correlations, one must understand and control the evolution of the crystallinity with the intrinsic gel texture. Indeed, the crosslinking process may have opposite effects with respect to the two processes that govern polymer crystallinity: nucleation may be favoured by introduction of a small amount of crosslinks which could play the role of impurities

whereas growth should be hindered by the decrease of molecular mobility induced by gelation. Moreover, macromolecules possess a very long temporal memory of their thermal and dynamic history. Therefore, any quantitative correlation of crystallinity with network structure should be attempted only after the physical mechanisms of crystallization of these systems have been studied by carefully controlling the experimental thermodynamic conditions.

A second point concerns the physical origin of the relation structural–transport properties. As the gels lose their crystallinity upon doping, the existence of a correlation between conducting clusters of doped systems and crystalline domains of undoped polymers, often evoked in the literature but still unproved, may imply that a memory of the crystalline domains persists in the non-crystalline doped structure. Partial chain organization would therefore exist in small zones which would present an enhanced conductivity.

Conclusion

The results presented here show that the crosslinking process can be used to modulate and enhance the transport properties and the state of crystallinity of POT gels. The description of the semi-crystalline state in relation to the crosslink density as well as the physical mechanisms of correlation of structure/large-scale heterogeneities and structure/transport have to be refined. This will be presented in subsequent work using coupled n.m.r., X-ray diffraction, conductivity and SAXS techniques to approach the ultimate aim: to be able to modulate the conduction by varying the specific degree of freedom of networks, the crosslink density.

Acknowledgements

We would like to thank the European Synchrotron Radiation Facilities (ESRF, Grenoble, France) for making the beam time available. We also thank J. P. Simon for his help and assistance with the SAXS spectrometer on D2AM.

References

1. Viallat, A. and Pépin-Donat, B., *Macromolecules*, 1997, **30**(16), 4679.
2. Sixou, B., Pépin-Donat, B. and Nechtschein, M., *Polymer*, 1997, **38**(7), 1581.
3. Weider H. H., Laboratory Notes on Electrical and Galvanometric Measurements, *Materials Science Monographs*, Vol. 2. Elsevier, New York, 1979, p. 5.
4. AFNOR (ed.), *Recueil des Normes Françaises*, 1987, p. 172.
5. Simon, J. P., Arnaud, F., Bley, F., Berar, J. F., Caillot, B., Comparat, Y. and Geissler, E., *J. Applied Cryst.*, 1997, **30**, 900.
6. Gustafsson, G., Inganas, O., Österholm, H. and Laasko, J., *Polymer*, 1991, **32**(9), 1574.
7. Alexander L. E., *X-ray Diffraction Methods in Polymer Science*. Wiley-Interscience, New York, 1976, Chapter 7.